species of zero bond order, which are either unbound or bound by dispersion in the absence of a magnetic field. This bonding is sufficiently strong to affect the chemistry of molecules in strong magnetic fields.

References and Notes

1. T. Helgaker, W. Klopper, D. P. Tew, *Mol. Phys.* **106**, 2107 (2008).
2. R. H. Garstang, *Rep. Prog. Phys.* **40**, 105 (1977).
3. S. Jordan, P. Schmelcher, W. Becken, W. Schweizer, *Astron. Astrophys.* **336**, L33 (1998).
4. S. Jordan, P. Schmelcher, W. Becken, *Astron. Astrophys.* **376**, 614 (2001).
5. D. Lai, *Rev. Mod. Phys.* **73**, 629 (2001).
6. M. Žaucer, A. Ažman, *Phys. Rev. A* **18**, 1320 (1978).
7. A. Kubo, *J. Phys. Chem. A* **111**, 5572 (2007).
8. Y. E. Lozovik, A. V. Klyuchnik, *Phys. Lett. A* **66**, 282 (1978).
9. S. Basile, F. Trombetta, G. Ferrante, *Nuovo Cim.* **9**, 457 (1987).
10. P. J. Knowles, N. C. Handy, *Chem. Phys. Lett.* **111**, 315 (1984).
11. W. Duch, *GRMS or Graphical Representation of Model Spaces I: Basics* (Springer-Verlag, New York, 1986).
12. J. Olsen, B. O. Roos, P. Jørgensen, H. J. A. Jensen, *J. Chem. Phys.* **89**, 2185 (1988).
13. T. Helgaker, P. Jørgensen, J. Olsen, *Molecular Electronic-Structure Theory* (Wiley, Chichester, UK, 2000).
14. P. Schmelcher, L. S. Cederbaum, *Phys. Rev. A* **41**, 4936 (1990).
15. F. London, *J. Phys. Radium* **8**, 397 (1937).
16. R. Ditchfield, *J. Chem. Phys.* **56**, 5688 (1972).
17. K. Wolinski, J. F. Hinton, P. Pulay, *J. Am. Chem. Phys. Soc.* **112**, 8251 (1990).
18. W. Kutzelnigg, *Isr. J. Chem.* **19**, 193 (1980).
19. M. Schindler, W. Kutzelnigg, *J. Chem. Phys.* **76**, 1919 (1982).
20. U. Kappes, P. Schmelcher, *Phys. Lett. A* **210**, 409 (1996).
21. U. Kappes, P. Schmelcher, *Phys. Rev. A* **53**, 3869 (1996).
22. U. Kappes, P. Schmelcher, *Phys. Rev. A* **54**, 1313 (1996).
23. E. I. Tellgren, A. Soncini, T. Helgaker, *J. Chem. Phys.* **129**, 154114 (2008).
24. E. I. Tellgren, T. Helgaker, A. Soncini, *Phys. Chem. Chem. Phys.* **11**, 5489 (2009).
25. P. K. Kennedy, D. H. Kobe, *Phys. Rev. A* **30**, 51 (1984).
26. T. H. Dunning, *J. Chem. Phys.* **90**, 1007 (1989).
27. D. E. Woon, T. H. Dunning, *J. Chem. Phys.* **100**, 2975 (1994).
28. P. Schmelcher, L. S. Cederbaum, *Phys. Rev. A* **37**, 672 (1988).
29. U. Kappes, P. Schmelcher, *J. Chem. Phys.* **100**, 2878 (1994).
30. M. Jeziorska, W. Cencek, K. Patkowski, B. Jeziorski, K. Szalewicz, *J. Chem. Phys.* **127**, 124303 (2007).

Acknowledgments: Supported by the Norwegian Research Council through Centre for Theoretical and Computational Chemistry (CTCC) grant 179568/V30 and through grant 197446/V30 and by the European Research Council (ERC) under the European Union's Seventh Framework Program through the advanced grant ABACUS, ERC grant agreement 267683. M.R.H. acknowledges support from the CTCC during a sabbatical stay at the University of Oslo in 2010.

26 January 2012; accepted 25 May 2012
10.1126/science.1219703

Sulfate Burial Constraints on the Phanerozoic Sulfur Cycle

Itay Halevy,[1,2]* Shanan E. Peters,[3] Woodward W. Fischer[2]

The sulfur cycle influences the respiration of sedimentary organic matter, the oxidation state of the atmosphere and oceans, and the composition of seawater. However, the factors governing the major sulfur fluxes between seawater and sedimentary reservoirs remain incompletely understood. Using macrostratigraphic data, we quantified sulfate evaporite burial fluxes through Phanerozoic time. Approximately half of the modern riverine sulfate flux comes from weathering of recently deposited evaporites. Rates of sulfate burial are unsteady and linked to changes in the area of marine environments suitable for evaporite formation and preservation. By contrast, rates of pyrite burial and weathering are higher, less variable, and largely balanced, highlighting a greater role of the sulfur cycle in regulating atmospheric oxygen.

Sulfate (SO_4^{2-}) is the fourth most abundant ion in modern seawater and a major component of the alkalinity budget, which governs the pH of seawater (*1*). Bacterial sulfate reduction accounts for ~50% of sedimentary organic matter respiration (*2*), and precipitation of pyrite (FeS_2) is one of the major exit channels of sulfur from the ocean (*3*). Because reduction of riverine sulfate and burial of the sulfide leave oxidized products in the ocean-atmosphere system, pyrite burial is considered a major indirect source of oxygen to the atmosphere (*4*, *5*).

Several time series data sets constrain aspects of the Phanerozoic sulfur cycle (Fig. 1A). The sulfur isotope composition, $\delta^{34}S$, of carbonate-associated sulfate, sulfate evaporites, and barite ($BaSO_4$) records the $\delta^{34}S$ of seawater sulfate, whereas the $\delta^{34}S$ of sedimentary pyrite captures the products of microbial sulfate reduction (*6*–*8*). The chemical composition of fluid inclusions in halite constrains the concentration of major ions in seawater, including sulfate (*9*, *10*).

Variability in the $\delta^{34}S$ records of seawater sulfate and sedimentary pyrite is typically interpreted to reflect changes in the fraction of sulfur removed from the oceans as pyrite, f_{pyr}. Because pyrite is depleted in ^{34}S by several percent relative to the sulfate reservoir from which it formed, times of high seawater sulfate $\delta^{34}S$ are interpreted as times of high rates of pyrite burial. By assuming a steady state and constant input magnitude and $\delta^{34}S$, or by scaling inputs and outputs to modern values, models of the Phanerozoic sulfur cycle explain long-term trends in $\delta^{34}S$ values by changes in f_{pyr} between ~0.2 and ~0.6 (*4*, *11*–*13*). Recognizing that the magnitude and $\delta^{34}S$ of the influxes to the ocean have likely varied in time, thereby influencing the isotopic record, some models included parameterized influxes and solved mass balance equations for the outfluxes and the value of f_{pyr} (*4*, *13*). The parameterizations are uncertain, however, because they are largely based on a scaling of modern influxes by debated factors, such as the relative rates of seafloor spreading and continental runoff (*14*, *15*).

It is possible to measure the sink of sulfate evaporites from seawater and obtain estimates of the influx magnitude and $\delta^{34}S$ by mass balance, though previous volume estimates of Phanerozoic evaporites (mostly halite, but some sulfate) have been considered too coarse or uncertain to accurately constrain past rates of sulfate burial (*16*–*18*). We quantified sulfate burial over Phanerozoic time, using a comprehensive macrostratigraphic database (*19*, *20*), which includes 23,843 lithostratigraphic rock units in 949 geographic locations across North America and the Caribbean (NAC). Data were binned by age, and sulfate burial rates were obtained by dividing evaporite volume by bin duration. Macrostratigraphy-based estimates of sulfate burial rates are higher than those derived from other compilations. This is due to the improved spatial and lithological resolution of this data set, which includes sedimentary rocks in the surface and subsurface, and many comparatively thin but widespread deposits not included in previous compilations. Notably, the NAC burial rates are highly variable, with values 2 to 14 times the average occurring mainly in Paleozoic intervals (Fig. 1C).

The macrostratigraphic database currently provides comprehensive coverage only in NAC, but can be scaled globally (Fig. 1D) by using mechanistic relationships between the observations and environmental controls on sulfate evaporite deposition (*20*). The volume-weighted average ratio of global to North American sulfate deposit volumes is ~8 (*16*, *17*). In comparison, the area-weighted ratio of global to NAC submerged continental area in latitudes of net evaporation, estimated from paleogeographic reconstructions (*20*, *21*), is ~7. This close agreement reflects a primary requirement for massive sulfate evaporite deposition—hydrographic isolation of large, marine-fed basins at latitudes of net evaporation (*22*). Such basins are created by rifting, small changes in sea level or the development of a barrier to circulation (*22*), often at the shoreward edge of submerged continental shelves. Indeed,

[1]Environmental Sciences and Energy Research, Weizmann Institute of Science, Rehovot 76100, Israel. [2]Geological and Planetary Sciences, California Institute of Technology, Pasadena, CA 91125, USA. [3]Geoscience, University of Wisconsin-Madison, Madison, WI 53706, USA.

*To whom correspondence should be addressed. E-mail: itay.halevy@weizmann.ac.il

the long time-scale variability in the burial rate data is well explained by the estimated NAC submerged continental area at latitudes ±10° to 50° (linear product moment correlation coefficient of 0.47 at the temporal resolution of the paleogeographic reconstructions), and we use this relationship to derive average global burial rates. We add shorter time scale variability to this average using correlations between NAC fluxes and the rate of change in eustatic sea level (*20*, *23*). Additional factors that influence evaporite deposition, such as geodynamic controls on basin subsidence and climate patterns at the regional-to-local scale (*22*), are not explicitly represented by this scaling methodology. They are, however, implicitly included in the scaling because they have contributed to the observed NAC sulfate burial rates (*20*).

Intervals of rapid sulfate evaporite burial (NAC and global) occur with equal frequency during times of high and low marine sulfate concentrations (Fig. 1). This reveals that sulfate burial rates were disconnected from changes in the activity product of calcium and sulfate [$aCa^{2+}aSO_4^{2-}$; e.g., (*13*)], which have varied by up to ~15% (*9*, *10*). We suggest, instead, that the first-order control on sulfate burial was the episodic availability of suitable environments in which evaporation of seawater could lead to saturation, precipitation, accumulation, and long-term preservation of sulfate evaporites. Unsteady sulfate burial rates, governed by the interactions between sea level, tectonics, and paleogeography, suggest that the critical statistic derived from isotope mass balance studies, f_{pyr}, convolves information regarding the relative activity of sulfate-reducing microbiota with the availability of environments suitable for sulfate burial. For example, a decrease in the area of shallow seas due to a drop in sea level or continental migrations could decrease sulfate burial rates and increase f_{pyr}. The rate of pyrite burial itself need not change. Scaled globally and corrected for the decay of surviving rock with time (*20*), the macrostratigraphic data reveal an average Phanerozoic sulfate evaporite burial rate of ~3.3×10^{11} to 4.5×10^{11} mol year^{-1}, depending on bin duration. This is only ~10 to 30% of the estimated riverine influx of sulfate to the oceans [~1.5×10^{12} to 3.5×10^{12} mol year^{-1}; (*12*, *24*)], implying that the value of f_{pyr} has been ~0.7 to 0.9 if the sulfur cycle operated close to steady state.

The macrostratigraphic data motivated us to reevaluate models of the sulfur cycle by integrating constraints from sulfur isotope measurements and sulfate concentration data from fluid inclusions. In any isotope mass balance model, the time-dependent concentration and $\delta^{34}S$ of seawater sulfate can be expressed by two equations

$$\frac{dM}{dt} = J_{in} - J_e - J_p \quad (1)$$

$$\frac{dM\delta}{dt} = J_{in}\delta_{in} - J_e\delta - J_p(\delta - \Delta) \quad (2)$$

Here, M is the concentration of seawater sulfate and δ is its $\delta^{34}S$ value. J_{in} is the total influx of sulfur to the oceans, with contributions from evaporite weathering, oxidative weathering of sedimentary and igneous sulfide minerals, and volcanic outgassing of sulfur volatiles. The $\delta^{34}S$ of this influx, δ_{in}, depends on the relative contributions of these three components. J_e and J_p are the burial fluxes of sulfate evaporites and pyrite, respectively, and Δ is the average difference (in permil) between the $\delta^{34}S$ of contemporaneous sulfate evaporite and pyrite sedimentary sinks. The values of M, δ, and Δ can be constrained by $\delta^{34}S$ and fluid inclusion data, and J_e, by macrostratigraphic data.

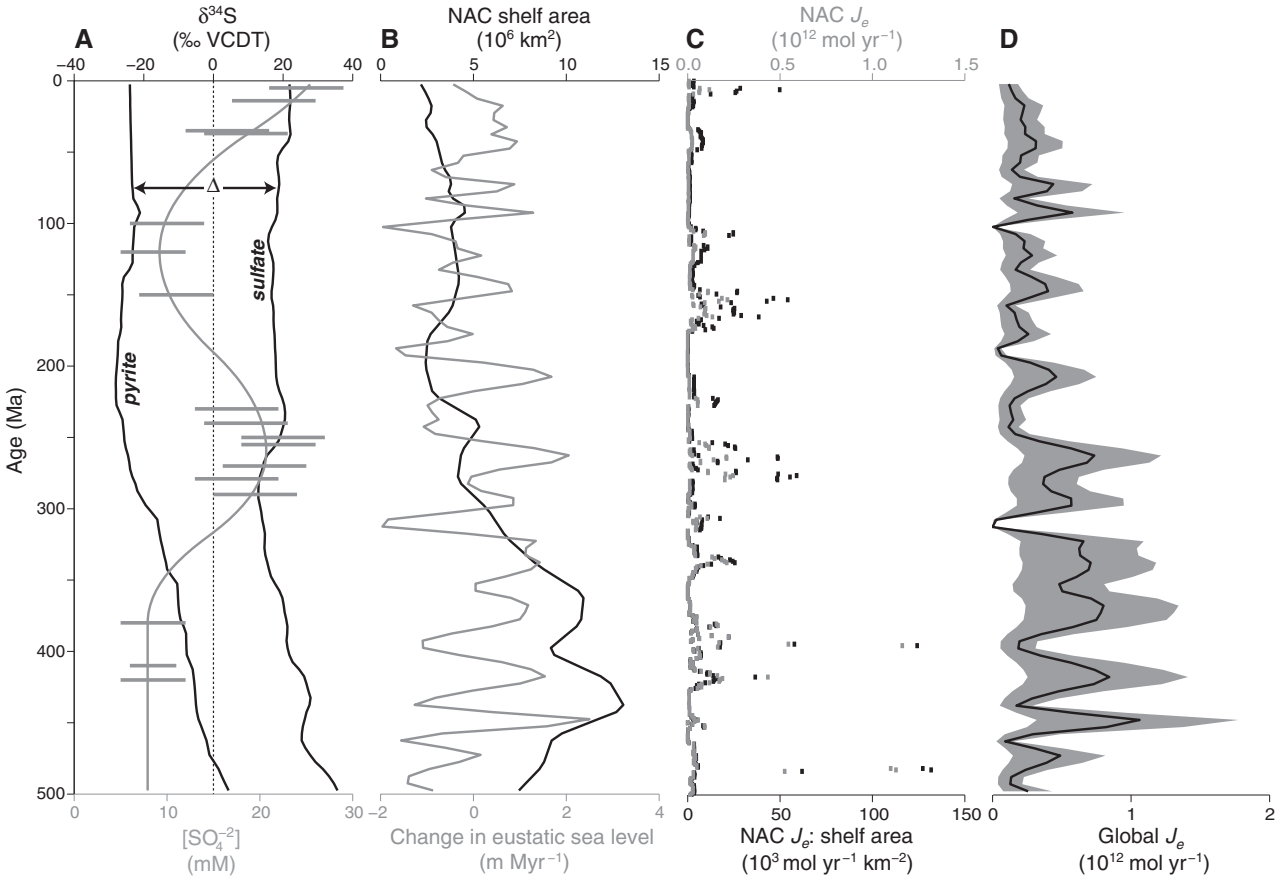

Fig. 1. Observational constraints on the Phanerozoic sulfur cycle. (**A**) Sulfur isotope composition of seawater sulfate and sedimentary pyrite (*8*), and seawater sulfate concentration from fluid inclusions in halite (*9*, *10*). Isotope compositions are reported relative to the standard VCDT (Vienna Canyon Diablo Troilite). (**B**) North America and the Caribbean (NAC) submerged continental area estimates and the rate of change of global mean sea level (*23*). (**C**) Estimates of NAC total and per-area sulfate evaporite burial rates. (**D**) NAC sulfate evaporite burial rates scaled to global fluxes and corrected for decay of the surviving record (*20*), including uncertainty (shaded envelope).

It is possible to solve Eqs. 1 and 2 for the outputs using the inputs ("parameterized input") or for the inputs using the outputs ("parameterized output"), and the solutions can be evaluated with independent physical understanding of the sulfur cycle. We examined three variants of the parameterized input model (*20*). The first assumed constant values of J_{in}, δ_{in}, and Δ (*11*, *12*, *24*) and either a steady state or a dynamic mass balance. In the second and third models, we used influx parameterizations similar to those of (*18*) and (*13*). We examined three variants of the parameterized output model (*20*). The first is a model of constant f_{pyr}. The second, motivated by the observation that pyrite burial is common in shallow, organic-rich sediments (*25*), is a model in which J_p scales with normalized global submerged continental area. This scaling may be weak because although high submerged areas may lead to high bacterial sulfate reduction rates, inefficient delivery of reactive iron across the shelf could limit pyrite burial to near-shore environments (*26*). We therefore considered a third model of constant J_p. Using the macrostratigraphy-based sulfate burial rates as additional constraints, we solved Eqs. 1 and 2 for the time-dependent values of J_{in} and δ_{in}.

Of the parameterized output models (Fig. 2, A to C), the models of constant f_{pyr} yield unrealistically low values of J_{in} (often lower than estimates of the volcanic influx and occasionally negative) and wildly varying values of δ_{in}. The latter is related to the former; if J_{in} is small, then the change in δ_{in} required to drive an observed change in seawater sulfate $\delta^{34}S$ must be large. The models of submerged continental area-dependent or constant J_p yield reasonable values of J_{in} and low values of δ_{in} (near the average sedimentary pyrite $\delta^{34}S$) that become higher during times of increased J_e. This is consistent with the idea of rapid sediment recycling (*4*), where low values of δ_{in} closely follow high relative rates of pyrite burial due to oxidative weathering of recently deposited pyrite; high δ_{in} values result from weathering of newly deposited sulfates. Notably, dynamic and steady-state solutions diverge only during short intervals of rapid change in seawater sulfate concentrations, implying that the system operates much of the time close to steady state. All three parameterized output models, when constrained by the macrostratigraphic data, indicate high average values of f_{pyr} (~0.7 to 0.9).

The parameterized input models yield values of f_{pyr} similar to those in previous modeling studies of the Phanerozoic sulfur cycle (Fig. 2, D and F). However, the model of constant δ_{in} at steady state occasionally requires unrealistically low values of J_{in} to reproduce the $\delta^{34}S$ records [Fig. 2E; e.g., 200 Ma (millions of years ago)], supporting the notion that the $\delta^{34}S$ value of inputs has varied with time. The values of J_e required for mass balance under the other parameterizations are ~three times as large as our burial rate estimates (Fig. 2, E and G, and fig. S1). We hypothesize that this is because parameterizations for the sulfate influx into the ocean are calibrated to modern riverine fluxes, which are higher than the expected long-term average due to the exposure and weathering of recently deposited evaporites (supplementary text). This notion is supported by anomalously high per-area sulfate deposition rates obtained from the NAC macrostratigraphic compilation during the last 10 million years (Fig. 1C); by widespread massive Neogene-age (~23 to 2.6 Ma) evaporites in Europe, Asia, and Africa (*22*, *27*–*31*); and by the recognition that deposition rates decrease with increasing observation time scale to constant, long-term values (*32*). This implies that the high abundance of Neogene-age sulfate evaporites represents gross deposition. Ultimately much of this material will not be preserved, and net deposition rates will converge to long-term Phanerozoic rates (*33*).

The results presented here describe a Phanerozoic sulfur cycle in which the majority of net inputs and outputs are oxidative weathering and burial of sedimentary pyrite, respectively. Over the time intervals resolved by our macrostratigraphic data, the long-term value we estimate for f_{pyr} is generally high, and large downward excursions in its value are associated with high rates of sulfate evaporite burial, rather than times of less pyrite burial. Although spatial heterogeneity and short–time scale variability in the value of J_p have likely occurred (*34*), global models of constant or slowly varying J_p (in response to changes in sub-

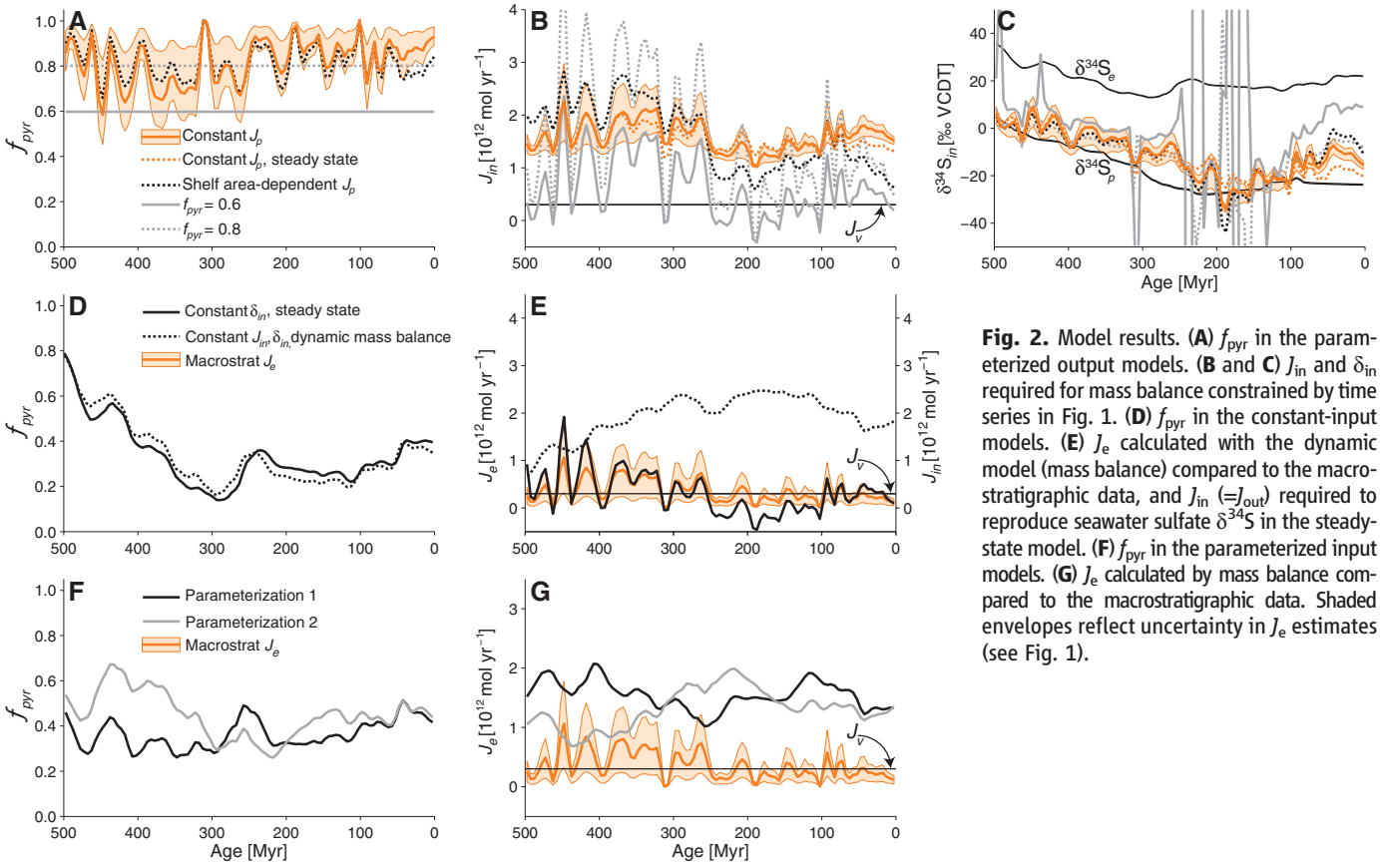

Fig. 2. Model results. (**A**) f_{pyr} in the parameterized output models. (**B** and **C**) J_{in} and δ_{in} required for mass balance constrained by time series in Fig. 1. (**D**) f_{pyr} in the constant-input models. (**E**) J_e calculated with the dynamic model (mass balance) compared to the macrostratigraphic data, and J_{in} (=J_{out}) required to reproduce seawater sulfate $\delta^{34}S$ in the steady-state model. (**F**) f_{pyr} in the parameterized input models. (**G**) J_e calculated by mass balance compared to the macrostratigraphic data. Shaded envelopes reflect uncertainty in J_e estimates (see Fig. 1).

merged continental area) yield results that are consistent both internally and with existing observations of seawater sulfate concentration and $\delta^{34}S$. Large and stable pyrite weathering and burial fluxes highlight the importance of oxidation-reduction feedbacks between carbon, iron, and sulfur (*24*) and imply a greater role for the sulfur cycle in regulating Phanerozoic atmospheric oxygen.

References and Notes

1. F. M. M. Morel, J. G. Hering, *Principles and Applications of Aquatic Chemistry* (Wiley, New York, 1993).
2. B. B. Jørgensen, *Nature* **296**, 643 (1982).
3. R. A. Berner, *Geochim. Cosmochim. Acta* **48**, 605 (1984).
4. R. A. Berner, *Am. J. Sci.* **287**, 177 (1987).
5. D. E. Canfield, *Annu. Rev. Earth Planet. Sci.* **33**, 1 (2005).
6. $\delta^{34}S = ({}^{34}R_{sam}/{}^{34}R_{ref} - 1) \times 1000$, where ${}^{34}R$ is the ratio of ${}^{34}S$ to ${}^{32}S$.
7. H. Strauss, *Palaeogeogr. Palaeocl.* **132**, 97 (1997).
8. N. P. Wu, J. Farquhar, H. Strauss, S. T. Kim, D. E. Canfield, *Geochim. Cosmochim. Acta* **74**, 2053 (2010).
9. T. K. Lowenstein, M. N. Timofeeff, S. T. Brennan, L. A. Hardie, R. V. Demicco, *Science* **294**, 1086 (2001).
10. J. Horita, H. Zimmermann, H. D. Holland, *Geochim. Cosmochim. Acta* **66**, 3733 (2002).
11. R. M. Garrels, A. Lerman, *Am. J. Sci.* **284**, 989 (1984).
12. D. E. Canfield, *Am. J. Sci.* **304**, 839 (2004).
13. A. Kampschulte, H. Strauss, *Chem. Geol.* **204**, 255 (2004).
14. D. B. Rowley, *Geol. Soc. Am. Bull.* **114**, 927 (2002).
15. J. M. Edmond, Y. Huh, in *Tectonic Uplift and Climate Change*, W. F. Ruddiman, W. Prell, Eds. (Plenum, New York, 1997), pp. 329–351.
16. A. B. Ronov, *Int. Geol. Rev.* **24**, 1313 (1982).
17. M. A. Zharkov, *History of Paleozoic Salt Accumulation*, A. L. Yanshin, Ed. (Springer, New York, 1981).
18. R. A. Berner, *Am. J. Sci.* **304**, 438 (2004).
19. S. E. Peters, N. A. Heim, *Paleobiology* **36**, 61 (2010).
20. Methods are available on *Science* Online.
21. C. R. Scotese, *Atlas of Earth History* (PALEOMAP Project, Arlington, TX, 2001).
22. J. K. Warren, *Earth Sci. Rev.* **98**, 217 (2010).
23. B. U. Haq, A. M. Al-Qahtani, *GeoArabia* **10**, 127 (2005).
24. L. R. Kump, R. M. Garrels, *Am. J. Sci.* **286**, 337 (1986).
25. D. E. Canfield, R. Raiswell, *Am. J. Sci.* **299**, 697 (1999).
26. R. Raiswell, *Elements* **7**, 101 (2011).
27. J. M. Rouchy, D. Noel, A. M. A. Wali, M. A. M. Aref, *Sediment. Geol.* **94**, 277 (1995).
28. T. M. Peryt, *Sediment. Geol.* **188–189**, 379 (2006).
29. W. Krijgsman, F. J. Hilgen, I. Raffi, F. J. Sierro, D. S. Wilson, *Nature* **400**, 652 (1999).
30. J. M. Rouchy, A. Caruso, *Sediment. Geol.* **188–189**, 35 (2006).
31. H. Rahimpour-Bonab, Z. Shariatinia, M. G. Siemann, *Geol. J.* **42**, 37 (2007).
32. P. M. Sadler, *GeoResearch Forum* **5**, 15 (1999).
33. S. E. Peters, *J. Geol.* **114**, 391 (2006).
34. B. C. Gill *et al.*, *Nature* **469**, 80 (2011).

Acknowledgments: We thank D. Canfield and J. Adkins for helpful discussion, and C. Scotese for help with the paleogeographic reconstructions. I.H. acknowledges support from a Texaco Postdoctoral Fellowship in Geological and Planetary Sciences at the California Institute of Technology and a Sir Charles Clore Prize for Outstanding Appointment in the Experimental Sciences at the Weizmann Institute of Science. S.E.P. was funded by NSF grant EAR-0819931. W.W.F. acknowledges support from the Agouron Institute and a David and Lucile Packard Foundation Fellowship for Science and Engineering. The binned macrostratigraphic data are available as a supplementary table on *Science* Online.

Supplementary Materials

www.sciencemag.org/cgi/content/full/337/6092/331/DC1
Materials and Methods
Supplementary Text
Figs. S1 to S5
References (*35–46*)
Database S1

7 February 2012; accepted 5 June 2012
10.1126/science.1220224

Rapid Variability of Seawater Chemistry Over the Past 130 Million Years

Ulrich G. Wortmann[1]* and Adina Paytan[2]*

Fluid inclusion data suggest that the composition of major elements in seawater changes slowly over geological time scales. This view contrasts with high-resolution isotope data that imply more rapid fluctuations of seawater chemistry. We used a non–steady-state box model of the global sulfur cycle to show that the global $\delta^{34}S$ record can be explained by variable marine sulfate concentrations triggered by basin-scale evaporite precipitation and dissolution. The record is characterized by long phases of stasis, punctuated by short intervals of rapid change. Sulfate concentrations affect several important biological processes, including carbonate mineralogy, microbially mediated organic matter remineralization, sedimentary phosphorous regeneration, nitrogen fixation, and sulfate aerosol formation. These changes are likely to affect ocean productivity, the global carbon cycle, and climate.

The chemical composition and mineralogy of skeletal limestones and biogenic carbonates vary systematically through time, indicating that the Mg/Ca ratio as well as other constituents of seawater have also changed (*1*). Fluid inclusion studies are also consistent with variable magnesium, calcium, sodium, and sulfate concentrations through time (*2*, *3*). Several hypotheses have been proposed to explain these secular trends, including changes in global weathering patterns (*4*), sea-floor spreading rates (*5*), or burial rates of these elements (*6*).

Evaporites play an important role in the latter process because their precipitation/dissolution rates exceed those of other sediments by three orders of magnitude (*7*, *8*). Halite is the dominant evaporite phase, but the effect of halite precipitation/dissolution on seawater chemistry is limited because the marine Na^+ and Cl^- reservoirs are large ($\approx 6.47 \times 10^{20}$ and 7.5×10^{20} mol respectively). Sulfur-bearing evaporites (such as $CaSO_4$) comprise on average 20% of an evaporite sequence (*9*) but have a 20 times smaller marine reservoir size than that of Cl^-.

The role of sulfur-bearing salts in controlling seawater chemistry is often overlooked. In the modern ocean, pyrite burial is not limited by sulfate availability (*10*), and the strong link between pyrite burial rates and sulfate concentration has just recently been recognized (*11*). Furthermore, basin-scale evaporites (BSEs) occur only sporadically in the geologic record and are not always visible, and the chemical composition of seawater does not depend on the mass of existing evaporites (Fig. 1A) but on the amount of salts that have already been eroded (Fig. 1B) and/or were originally extracted (Fig. 1C). The past 130 million years saw only two BSE events (Fig. 1C): one caused by the desiccation of the Mediterranean during the Messinian (*12*), and the second related to the Early Cretaceous opening of the South Atlantic (*11*, *12*).

Until recently, all available data supported the assumption of slow secular changes to major seawater constituents and their related biogeochemical fluxes. However, as the temporal resolution of proxy data increases, it becomes evident that the rate of change is often faster than expected from the residence time of major species.

High-resolution data sets of seawater $\delta^{34}S$ record two major events, at 130 to 120 million years ago (Ma) and 55 to 45 Ma, that require large changes to the S-fluxes and/or their isotopic composition. Previous interpretations of the $\delta^{34}S$ record called for changes in the planetary degassing flux and/or S burial rates (*6*). Clearly, volcanic activity and pyrite burial are major parameters, but we propose to broaden the discourse by including the effects of evaporite precipitation and dissolution. If these processes occur on a basin-wide scale, they will modify the flux and $\delta^{34}S$ of the sulfur input/output and change the marine sulfate concentration, which in turn affects pyrite burial in a nonlinear way (*11*), further affecting seawater isotopic composition. Under modern conditions, this effect is negligible. However, with decreasing sulfate concentrations, the importance of sulfate availability increases until it becomes the dominant parameter controlling pyrite burial (*11*).

[1]Geobiology Isotope Laboratory, Department of Geology, University of Toronto, Toronto, ON M5S 3B1, Canada. [2]Institute of Marine Sciences University of California Santa Cruz, Santa Cruz, CA 95064, USA.

*To whom correspondence should be addressed. E-mail: uli.wortmann@utoronto.ca (U.G.W.); apaytan@ucsc.edu (A.P.)